JB
Journals.ASM.org

The Sulfur Oxygenase Reductase from the Mesophilic Bacterium *Halothiobacillus neapolitanus* Is a Highly Active Thermozyme

Andreas Veith,[a] Hugo M. Botelho,[b] Florian Kindinger,[a] Cláudio M. Gomes,[b] and Arnulf Kletzin[a]

Institute of Microbiology and Genetics, Technische Universität Darmstadt, Darmstadt, Germany,[a] and Instituto de Tecnologia Química e Biológica, Universidade Nova de Lisboa, Oeiras, Portugal[b]

A biochemical, biophysical, and phylogenetic study of the sulfur oxygenase reductase (SOR) from the mesophilic gammaproteobacterium *Halothiobacillus neapolitanus* (*Hn*SOR) was performed in order to determine the structural and biochemical properties of the enzyme. SOR proteins from 14 predominantly chemolithoautotrophic bacterial and archaeal species are currently available in public databases. Sequence alignment and phylogenetic analysis showed that they form a coherent protein family. The *Hn*SOR purified from *Escherichia coli* after heterologous gene expression had a temperature range of activity of 10 to 99°C with an optimum at 80°C (42 U/mg protein). Sulfite, thiosulfate, and hydrogen sulfide were formed at various stoichiometries in a range between pH 5.4 and 11 (optimum pH 8.4). Circular dichroism (CD) spectroscopy and dynamic light scattering showed that the *Hn*SOR adopts secondary and quaternary structures similar to those of the 24-subunit enzyme from the hyperthermophile *Acidianus ambivalens* (*Aa*SOR). The melting point of the *Hn*SOR was ≈20°C lower than that of the *Aa*SOR, when analyzed with CD-monitored thermal unfolding. Homology modeling showed that the secondary structure elements of single subunits are conserved. Subtle changes in the pores of the outer shell and increased flexibility might contribute to activity at low temperature. We concluded that the thermostability was the result of a rigid protein core together with the stabilizing effect of the 24-subunit hollow sphere.

Sulfur oxygenase reductases (SORs) catalyze a dioxygen-dependent disproportionation reaction of elemental sulfur with sulfite, thiosulfate, and sulfide as products. External cofactors or electron donors are not required, and the two enzyme activities could not be separated (equations 1 to 3) (19, 20, 30, 41).

$$\text{Oxygenase} \quad S^0 + O_2 + H_2O \rightarrow HSO_3^- + H^+ \tag{1}$$

$$\text{Disproportionation} \quad 3S^0 + 3H_2O \rightarrow 2H_2S + HSO_3^- + H^+ \tag{2}$$

$$\text{Sum} \quad 4S^0 + O_2 + 4H_2O \rightarrow 2H_2S + 2HSO_3^- + 2H^+ \tag{3}$$

Thiosulfate is formed rapidly and in a pH-dependent manner from sulfite and excess sulfur at elevated temperatures (equation 4) (20, 33), but it is not yet known whether it is a primary reaction product as well.

$$\text{Thiosulfate formation} \quad S^0 + HSO_3^- \xrightarrow[pH < 4]{pH > 6} SSO_3^{2-} \tag{4}$$

SOR is the initial sulfur-oxidizing enzyme in the chemolithoautotrophic and thermoacidophilic archaea *Acidianus ambivalens* (*Aa*SOR) and *Acidianus tengchongensis* (*At*SOR), which grow optimally at 70 to 80°C and pH 1 to 4. The three-dimensional (3D) structures of both highly similar SORs (88% identity) showed that the enzymes form large spherical, hollow oligomers with molecular masses of 845 kDa each composed of 24 identical subunits (25, 46). Each subunit contains a low-potential mononuclear nonheme iron site as the putative redox-active cofactor and an indispensable cysteine, which is persulfurated in the *Ac. ambivalens* SOR (C31) (25, 45, 46). The iron sites are located in smaller pockets within each subunit, which are accessible only from the large inner cavity. We had shown using site-directed mutagenesis that the three Fe-coordinating residues (H_{86}, H_{90}, and E_{114}) and the persulfurated cysteine C_{31} are essential for catalysis. Most likely, the cysteine persulfide is involved in sulfur binding. Mutation of the other two cysteine residues in the protein did not abolish activity, not even in a double mutant (47). Our current hypothesis about the reaction mechanism of SOR predicts that the catalytic cycle is initiated by covalent sulfur binding to the active site C_{31} as a polysulfide chain (R-S_n-SH), followed by hydrolytic cleavage of the cysteine polysulfide to sulfide and a polysulfenyl moiety (R-S_n-SOH). Either the sulfenyl group or Fe^{2+} would subsequently activate dioxygen for polysulfenyl oxidation to the final product(s) sulfite and/or thiosulfate (19).

SORs or *sor* genes are not widespread in nature. So far, they have been reported only from some thermoacidophilic members of the domain *Archaea* and (hyper)thermophilic members of the domain *Bacteria*. Native SOR enzymes were initially purified from two *Acidianus* species (8, 20). Later, heterologous gene expression allowed study of the *Aa*SOR and *At*SOR in more detail (5, 41, 45). In addition, the SOR from the hyperthermophilic bacterium *Aquifex aeolicus* was biochemically characterized, resulting in similar properties compared to the *Aa*SOR and *At*SOR (30). Surprisingly, *sor* genes were recently found in the genomes of a number of mesophilic and moderately thermophilic bacteria, showing that SORs are not restricted to hyperthermophiles. The issue is relevant for enzymes metabolizing elemental sulfur because the water solubility of the barely soluble solid substrate decreases significantly with temperature (478 nM α-S_8 at 80°C to 6.1 nM at 4°C

Received 16 November 2011 **Accepted** 21 November 2011
Published ahead of print 2 December 2011
Address correspondence to Arnulf Kletzin, Kletzin@bio.tu-darmstadt.de.
Supplemental material for this article may be found at http://jb.asm.org/.

doi:10.1128/JB.06531-11

[15]), which raises the question whether substrate availability may limit enzyme activity at mesophilic conditions. There is one report of a SOR-like enzyme activity in soluble extracts of the mesophilic bacterium *Acidithiobacillus thiooxidans*, but molecular details were not given (43).

In order to investigate the structural and biochemical properties of SORs from a mesophile, we initiated a biochemical, biophysical, and enzymological study of the enzyme from the gammaproteobacterium *Halothiobacillus neapolitanus* (*Hn*SOR) to resolve this issue. The chemolithoautotrophic microbe grows optimally at 28 to 32°C at more or less neutral pH with thiosulfate or sulfur as electron donors (17). The type strain (NCIMB 8539) was isolated from corroded concrete sewers in Australia (29) and named "pertaining to the seawater at Naples from which this species was probably first isolated by Nathansohn in 1902" (18). It seems to be common in sulfide-rich spas and microbial leaching communities (3, 49). Apart from the *sor* gene, the *H. neapolitanus* genome encodes a complete SOX complex, a multisubunit sulfur oxidation complex restricted to *Bacteria* (10). The same applies to *Acidithiobacillus caldus.* It had been speculated that two sulfur-oxidizing enzyme systems might be used at different temperatures (26). *H. neapolitanus* does not grow at temperatures exceeding 42°C (18), and data regarding the temperature regulation effects, which are hypothetical so far, are lacking for both species.

We show here that recombinant *Hn*SOR is a highly active enzyme, with a very broad temperature spectrum of activity ranging from 10°C to more than 95°C. Also, the results of spectroscopy and *in silico* modeling suggest that the enzyme adopts secondary and quaternary structure similar to those from (hyper)thermophiles. The activity optimization of the *Hn*SOR is discussed as an apparent adaptive response to substrate limitation at mesophilic conditions, which allows efficient sulfur-based energy metabolism.

MATERIALS AND METHODS

Strain and culture conditions. *Halothiobacillus neapolitanus* DSM 15147 = NCIMB 8539 (1, 18) was obtained from the Deutsche Sammlung für Mikroorganismen und Zellkulturen (DSMZ; Braunschweig, Germany; http://www.dsmz.de). Cells were grown in liquid culture at 28 to 30°C either with 1% (wt/vol) tyndallized elemental sulfur or with 1% (wt/vol) thiosulfate as an electron donor at pH 6.8 in medium 68 recommended on the DSMZ web server (http://www.dsmz.de/catalogues/catalogue-microorganisms/culture-technology/list-of-media.html). Cells were grown until the color of bromocresol purple shifted to yellow, indicating a drop in pH, and subsequently harvested by centrifugation.

DNA procedures and heterologous gene expression. Isolation of chromosomal *H. neapolitanus* (DSM15147) DNA was carried out according to a modified protocol of *Sulfolobus solfataricus* DNA extraction by S. V. Albers (http://www.rug.nl/gbb/research/researchGroups/molecularMicrobiology/research/extremophiles/DNAsulf.pdf; as of November 2011). Six hundred micrograms of sedimented *H. neapolitanus* cells was resuspended in 550 μl of TEN buffer (40 mM Tris, 1 mM EDTA, 15 mM NaCl, pH 8). Fifty microliters of a 10% sodium dodecyl sulfate (SDS) (wt/vol) solution was added to the suspension, which was subsequently incubated for 45 min at room temperature. After repeated phenol-chloroform-isoamyl alcohol (25:24:1) and chloroform-isoamyl alcohol (24:1) extractions, the genomic DNA was precipitated by the addition of 0.1 volume of a 3 M sodium acetate solution (pH 5.2) and 0.8 volume of 2-propanol. After incubation at −20°C for 2 h, the tubes were centrifuged for 30 min at 16,000 × *g* in a microcentrifuge. The pelleted DNA was washed once with 70% ethanol (by volume), centrifuged for 5 min at 16,000 × *g*, dried at room temperature, and eventually resuspended in 50 μl of TE buffer (10 mM Tris, pH 8, 1 mM EDTA).

The *sor* gene (GenBank locus tag Hneap_1222) was PCR amplified with the primers *Hn*SOR_fwd (fwd stands for forward) (ACTAGT TA ACGA GGGCAA AAAATG TCGAAT GAAAAT CCAATT ATA) and *Hn*SOR_rev (rev stands for reverse) (GTGACG CCAAGC GCTTTG CT TAAG ATGCTT ACGCC) (Biomers, Ulm, Germany) which had been designed from the *H. neapolitanus* genome sequence (strain ATCC 23641). The PCR product was purified with the GenElute PCR clean-up kit (Sigma, Taufkirchen, Germany) according to the manufacturer's recommendations. It was subsequently cleaved with the SpeI and Eco47III restriction enzymes and ligated into the XbaI/Eco47III-digested pASK75 vector (38). Positive transformants in *Escherichia coli* Top 10F cells (Invitrogen, Darmstadt, Germany) were sequenced and finally introduced into *E. coli* BL21(DE3) CodonPlus RIL cells (Agilent, Böblingen, Germany).

For heterologous gene expression, 500-ml cultures were grown aerobically at 37°C in 2× LB medium in notched Erlenmeyer flasks. The expression was induced by the addition of 200 μg/liter anhydrotetracycline from a 2% (wt/vol) stock solution in dimethylformamide at an optical density at 600 nm (OD_{600}) between 0.6 and 0.8. Ferric citrate (100 μM) was added at the time of induction to ensure sufficient iron incorporation. The cultures were incubated for 20 h after induction with vigorous aeration and stirring. The *Acidianus ambivalens sor* gene (EMBL accession number X56616) was expressed heterologously after ligation into the pASK75 vector with a C-terminal Strep tag fusion (38) as described elsewhere (pASK-SOR.05 plasmid) (45).

Protein purification. The cell pellet obtained by centrifugation was washed once in approximately 10 volumes (vol/wt) of 100 mM Tris-HCl buffer (pH 8) with 150 mM NaCl (buffer W) and afterwards resuspended in 5 volumes of the same buffer. Cells were disrupted with a high-pressure homogenizer (0.18-mm nozzle and 1.35-MPa pressure; Constant Systems, Low March, Daventry, United Kingdom). After the first centrifugation step (10,000 × *g* for 30 min), the soluble protein-containing supernatant was centrifuged in an ultracentrifuge (100,000 × *g* for 45 min). The soluble total extract from 10 to 20 g of cells (wet weight) was applied either to a 1-ml Strep-Tactin gravity flow column or to an 8- to 10-ml Strep-Tactin superflow column (both columns from IBA, Göttingen, Germany) connected to an ÄKTApurifier 10 (GE Healthcare Bio-Sciences AB, Uppsala, Sweden). This step was performed repeatedly, when the binding capacity of the column was exceeded. The column was equilibrated with 5 column volumes (CV) of buffer W prior to loading. The column was subsequently washed with 6 CV of the same buffer. The protein was eluted by applying 3 CV of buffer E (buffer W with 2.5 mM desthiobiotin; IBA). The column was regenerated with 15 CV of buffer W with 1 mM hydroxyl-azophenyl benzoic acid (HABA) (Sigma). Alternatively, the column was regenerated with 3 CV each of double-distilled water (ddH_2O), 0.5 M NaOH, and ddH_2O instead of the regular HABA solution.

SOR activity and inhibition assays. The SOR activity assay was performed as previously described (20, 45). Specific activities were routinely determined after incubation of 0.5 to 5 μg of purified enzyme at 80°C in a 1-ml solution of 0.1 M sodium citrate–0.2 M Na_2HPO_4 (pH 7.2) (27) containing 2% sulfur (wt/vol) and 0.1% Tween 20 (vol/vol). Samples were taken at appropriate time points (usually after 0, 2, 4, 6, 8, and 10 min), chilled on ice, and centrifuged briefly to sediment elemental sulfur. The concentrations of the reaction products hydrogen sulfide, sulfite, and thiosulfate were determined colorimetrically (20) and quantified with calibration curves. The specific activities were calculated from the linear increase of the reaction products. One unit of enzyme activity was defined as 1 μmol of sulfite plus thiosulfate (oxygenase) or hydrogen sulfide (reductase) formed per minute.

The optimal pH and temperature of *Hn*SOR activity were determined with the same activity assay and different buffer systems. The citrate-phosphate buffer (27) was used to determine the protein activity in a range from pH 5 to 8. For higher pH values, 0.2 M Na_2HPO_4 was titrated with a

0.1 M Na_3PO_4 solution to the desired pH. The pH profile was recorded at 50°C due to extensive nonenzymatic sulfur disproportionation observed at high temperatures combined with high pH values (20, 40). Usually, 0.75 to 2.65 μg of purified *Hn*SOR was added to 1 ml of ice-cold assay buffer. The reaction was started by incubation of the tubes in a heating block at 50°C. The concentrations of reaction products and specific activities were determined as described above.

Different amounts of a freshly prepared $ZnCl_2$ solution resulting in a final concentration of 10 to 100 μM Zn^{2+} were added to the reaction mixtures in the SOR activity assay. The reaction mixture was kept on ice water for 30 min after 2 to 5 μg of enzyme had been added. The reaction was started by heating the samples to 80°C, and specific SOR activities were measured as described above. An enzymatic reaction mixture without $ZnCl_2$ and a nonenzymatic reaction mixture with inhibitor but without SOR were used as controls. For a second control, 2 mM EDTA was added to the zinc-containing reaction vials to reverse inhibition. All measured specific activities were plotted against the Zn^{2+} concentration. The slope of the trend line was used for calculation of the appropriate K_i values.

Biochemical procedures. The protein concentration was determined by the Coomassie blue method (2). Iron quantification was performed with pure protein preparations with the 2,4,6-tripyridyl-1,3,5-triazine (TPTZ) method (9). Denaturing SDS-polyacrylamide gel electrophoresis (PAGE) was performed with 10% or 12% polyacrylamide–Tris–tricine gels (35).

CD spectroscopy. Circular dichroism (CD) spectra were measured with a JASCO J-815 spectropolarimeter with Peltier temperature control. Typically, 10 accumulations were recorded in the far-UV region (180 to 260 nm) at 20°C with a data pitch of 0.2 nm and a 0.1-cm-path-length polarized quartz cuvette. A bandwidth of 2 nm was used with a detector response of 1 s and scanning speed of 200 nm/min. The spectra were obtained with 0.1 mg/ml of protein in 20 mM Tris-HCl buffer (pH 7.5) and afterwards corrected by subtracting the spectrum of the buffer solution. Thermal unfolding was assessed by measuring the CD signal at 220 nm while raising the temperature at a 1°C/min rate.

DLS. Dynamic light scattering (DLS) analyses of recombinant *Ac. ambivalens* and *H. neapolitanus* SORs were performed on a Zetasizer Nano apparatus (Malvern Instruments, Worcestershire, United Kingdom) at 25°C. Samples (0.3 mg/ml in 20 mM Tris-HCl buffer [pH 7.5]) were filtered through a 0.22-μm-pore-size filter and assayed with a quartz cuvette with 45-μl volume and 3-mm path length (Hellma, Müllheim, Germany). Three measurement cycles were performed for each protein sample. The data were averaged from 14 light scattering periods of 10 s for each cycle. Average protein diameter values were calculated using the corresponding Malvern Instruments DTS software.

Phylogenetic analysis and modeling. SOR homologues from other microorganisms were detected by BLASTP searches with the *Ac. ambivalens* SOR amino acid sequence as a probe (NCBI accession number CAA39952.1) against the public database at NCBI (www.ncbi.nlm.nih.gov). The deduced *Sulfobacillus* and *Acidithiobacillus ferrivorans* SOR sequences were identified via tBLASTN analysis in the respective genomes available at the DOE Joint Genome Institute (http://www.jgi.doe.gov). All SOR sequences were aligned by the KALIGN algorithm (24) with manual correction. The dendrogram was calculated feeding the alignment into the phylogeny server at the MAFFT site (http://mafft.cbrc.jp/alignment/server/phylogeny.html) with the default parameters and 100 bootstrap repetitions.

3D models of the *H. neapolitanus* SOR were predicted at the Phyre (http://www.sbg.bio.ic.ac.uk/phyre/html/index.html) (16) and I-Tasser servers (http://zhanglab.ccmb.med.umich.edu/I-TASSER/) (51). Energy minimization of the PHYRE model was performed with UCSF Chimera (http://www.cgl.ucsf.edu/chimera) (31). Clustering was done with CLUSPRO 2.0 (http://cluspro.bu.edu/login.php) (6, 22) and a single subunit in the dimer mode. Structure alignments, root mean square deviation (RMSD) readouts, and the preparation of figures were done with Pymol (7).

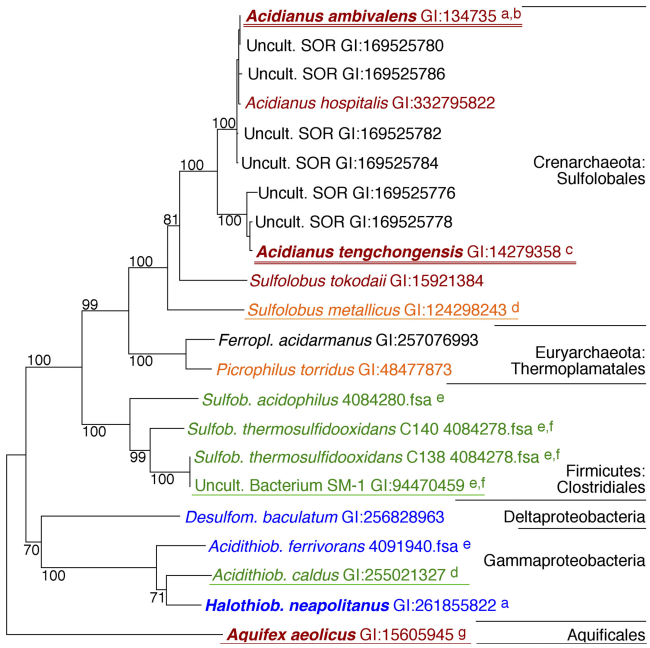

FIG 1 Color-coded phylogenetic dendrogram of the available SOR sequences in GenBank (GI numbers) (for alignment, see Fig. S1 in the supplemental material). The SOR sequences from uncultured (Uncult.) bacteria and other bacterial species, such as *Ferroplasma* (*Ferropl.*), *Sulfobacillus* (*Sulfob.*), *Desulfomicrobium* (*Desulfom.*), *Acidithiobacillus* (*Acidithiob.*), and *Halothiobacillus* (*Halothiob.*) species, are shown. Boldface type indicates that the SOR enzymes from this species were biochemically characterized. Underlining indicates that SOR activity was demonstrated in total cell extracts. Double underlining indicates that the X-ray structure is known. The numbers at the nodes of the dendrogram are bootstrap values. The optimal growth temperature is indicated by color as follows: red, optimal growth temperature of >70°C; orange, 51 to 70°C; green, 40 to 50°C; blue, ≈30°C; black, optimal growth temperature not known. Superscript letters a to d and g indicate the references as follows: a, this work; b, references 21 and 45; c, reference 41, d, reference 14; g, reference 30. The superscript e indicates that the sequence was retrieved from the web server of the Joint Genome Institute (http://www.jgi.doe.gov). The superscript f indicates that the two *sor* genes are located on different contigs of the *Sulfobacillus thermosulfidooxidans* genome sequence; they are identical to the two SOR SA and SB sequences obtained from a bioleaching reactor described in reference 5 and to the SOR sequence of the bacterium SM-1 described by the same authors.

RESULTS

Phylogenetic analysis of the SOR protein family. SORs form a conserved protein family with high mutual similarity (Fig. 1) (Pf07682; http://pfam.sanger.ac.uk) but with no recognizable similarity to outside proteins. The *Halothiobacillus neapolitanus* SOR (*Hn*SOR) shared pairwise amino acid identities with other SORs ranging between 76% (*Acidithiobacillus caldus*) and 40% (*Aquifex aeolicus*). The archaeal SORs were about 40 to 42% identical relative to the *Hn*SOR, while *Sulfobacillus* spp. (47%) were in between.

The aligned bacterial SOR amino acid sequences showed several regions with differences distinguishing them from the archaeal SORs (e.g., positions 91 to 96 and 112 to 117) (see Fig. S1 in the supplemental material). The dendrogram calculated from the alignment reflects a grouping of the enzymes according to phylo-

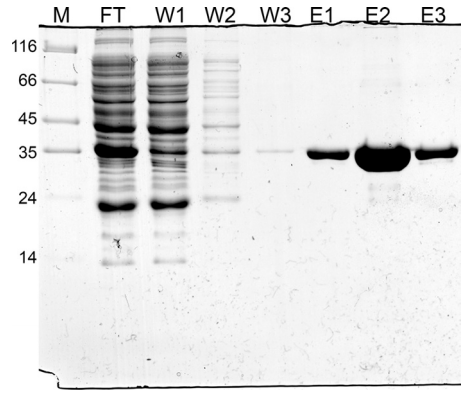

FIG 2 Coomassie blue-stained 12% polyacrylamide–Tris–Tricine–SDS gel of *Hn*SOR purified in a 1-ml Strep-Tactin gravity flow column. The protein was purified with 0.5-ml volume per wash/elution fraction according to the manufacturer's recommendation (IBA), and 10 μl of eluent was used per lane. Lanes; M, molecular mass markers; FT, flowthrough of *E. coli* soluble extract; W1 to W3, column wash fractions; E1 to E3, elution fractions. The positions of molecular mass markers (in kilodaltons) are indicated to the left of the gel.

genetic relationship (Fig. 1). The *Aquifex* SOR was always the least similar enzyme (33 to 40% identity) compared to all other SORs. It contained two insertions and a slightly shortened C terminus compared to the otherwise constant lengths of the SOR sequences. An outgroup was not included, as no paralogous sequence family with even minimal similarity was identified so far.

Cloning, expression, and purification of recombinant *H. neapolitanus* SOR. The *H. neapolitanus sor* gene (open reading frame [ORF] Hneap_1222) was cloned into the pASK75 expression vector with a C-terminal Strep tag (38). When sequenced for validation, the *sor* genes of strain DSM 15147 used here and of strain ATCC 23641 (genome sequence) were identical. When the resulting plasmid pASK_HnSOR was used to produce recombinant *Hn*SOR from *E. coli* BL21 cells, 20 to 30% of the protein was recovered in the soluble form, while the remainder precipitated in inclusion bodies. The purification yield was 11 to 18 mg of soluble protein per liter of 2× LB medium. SDS-PAGE revealed a major 36-kDa band characteristic of full-length SOR (Fig. 2). The average iron content of the preparations was 1.6 ± 0.3 Fe per protein monomer.

Enzymatic properties of recombinant *H. neapolitanus* SOR. The pH and temperature profiles of *Hn*SOR activity were determined with an enzyme buffer that was modified from those used previously for the *Acidianus* and *Aquifex* SORs (20, 30, 45). Optimal activity was observed when a 100 mM citrate-phosphate buffer was used (instead of Tris-acetate), resulting in 42.4 U/mg oxygenase and 4.1 U/mg reductase activities at pH 8 and 80°C. Both oxygenase and reductase activities were measured at temperatures between 10 and 95°C with an optimal activity at 80°C (Fig. 3B and C). At moderate temperatures (i.e., 10 to 40°C), both enzyme activities were at similar levels. At temperatures higher than 40°C, oxygenase activity was up to 10-fold higher than reductase activity. The same effect was previously observed for the *Aq. aeolicus* SOR (30). An equal ratio between both oxygenase products (sulfite and thiosulfate) was observed at moderate temperatures (10 to 40°C). The ratio drastically changed when temperatures exceeded 50°C, resulting in an up to sixfold-higher level of thiosulfate at 75°C.

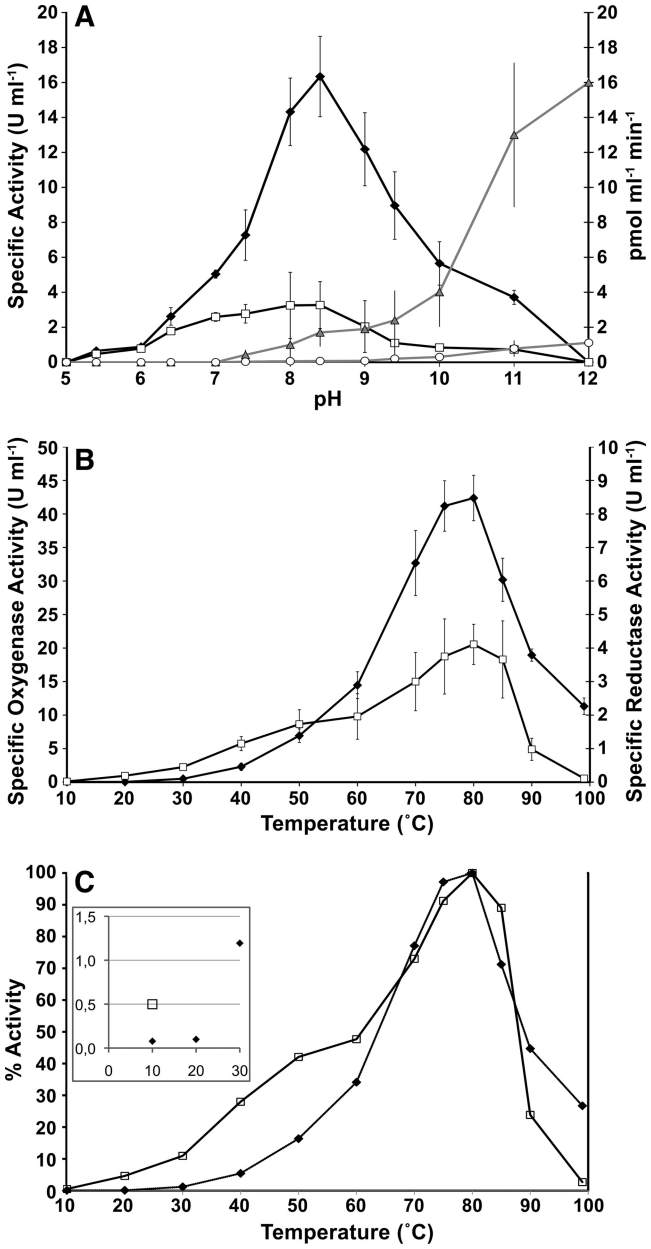

FIG 3 (A) pH dependence of *Hn*SOR activity recorded at 50°C. Specific enzyme activity is shown on the left-hand *y* axis (♦, sulfite plus thiosulfate production; □, H_2S production) Nonenzymatic sulfur disproportionation is shown on the right-hand *y* axis (▲, sulfite plus thiosulfate; ○, H_2S). (B) Temperature dependence of the specific activities of the *Halothiobacillus neapolitanus* SOR activity at pH 8. Sulfite plus thiosulfate production (♦) is shown on the left-hand *y* axis, and H_2S production (□) is shown on the right-hand *y* axis. (C) Relative specific activities as a percentage of the value at 80°C. Inset, enlargement of the 0 to 30°C range.

The activity assays used to determine the optimal pH for protein activity (Fig. 3A) were carried out at the suboptimal temperature of 50°C in order to avoid the interference of nonenzymatic sulfur disproportionation observed at higher temperatures combined with a pH of >8 (20, 40). Oxygenase and reductase activities were observed between pH 5.4 and 11 with an optimum at pH 8.4 (Fig. 3A). At pH 12, it was no longer possible to distinguish be-

TABLE 1 Properties of microorganisms and their sulfur oxygenase reductases[a]

Property[b]	*H. neapolitanus*[c]	*Aq. aeolicus*[d]	*Ac. ambivalens*[e]	*Ac. brierleyi*[f]	*Ac. tengchongensis*[g]
T_{opt} (°C)					
Microorganism	30	85	80	65–70	70
Enzyme	80	80	85	65	70
Sp act (U/mg) at T_{opt}					
Oxygenase	42.1	78.8	10.6	0.9	186.7
Reductase	4.1	3.05	2.6	NR	45.2
T range (°C) of enzyme	10–99	20–90	50–108	55–≥80	50–90
pH_{opt}					
Microorganism	6.5–6.9	6.8	2.5	1.5–2.0	2.5
Enzyme	8.4	NR	6.5–7.4	7.0	5
pH range of enzyme	5.4–11	5.5–8	5–8.4	NR	3.5–9
M_r					
Subunit	35,300	37,674	35,318	35,000[h]	35,172
Holoenzyme (method)	848,000 (DLS)	602,000 (native gel)	844,000 (X-ray)	560,000 (native gel)	845,000 (X-ray)
Zn^{2+} inhibition of oxygenase/reductase	K_i = 46/36 μM	NR	K_i = 45/39 μM	NR	27%[i]

[a] Properties of five microorganisms (*Halothiobacillus neapolitanus*, *Aquifex aeolicus*, *Acidianus ambivalens*, *Acidianus brierleyi*, and *Acidianus tengchongensis*) and their sulfur oxygenase reductases are shown.
[b] T_{opt}, optimum temperature; T range, temperature range; pH_{opt}, optimum pH; NR, not reported; DLS, dynamic light scattering.
[c] Data from this work.
[d] Data from reference 30.
[e] Data from references 20, 45, and 46.
[f] Data from reference 8.
[g] Data from references 11, 25, and 41.
[h] Apparent molecular mass on SDS gel; the gene is not known.
[i] Residual activity with 1 mM Zn^{2+}.

tween nonenzymatic sulfur disproportionation and the enzymatic reaction. Under slightly acidic conditions (pH 5.4 to 6.4), reductase and oxygenase activities were at comparable levels. The oxygenase and reductase activity ratios changed with increasing pH: at pH 7, a 2-fold excess of oxygenase over reductase activity was observed, which increased to almost 5-fold at the optimal pH of 8.4 (15.9 U/mg oxygenase and 3.27 U/mg reductase activities, respectively, at 50°C). Both products of the oxygenase reaction, sulfite and thiosulfate, were detected at all pH values tested. Sulfite was the major product under slightly acidic conditions (pH 5.4 to 6.4) (not shown). Thiosulfate formation was predominant under neutral and alkaline conditions: at pH 8, thiosulfate production was more than 3-fold higher than sulfite formation. The results are in agreement with the higher stability of thiosulfate at neutral and alkaline pH (equation 4).

The enzymatic activity of *Hn*SOR was lost when the protein or protein extracts were stored at −20°C. Consequently, preparations were kept either at 4°C or at −20°C after the addition of 50% glycerol, which prevented loss of activity. Previous reports about the *Aa*SOR and *At*SOR had shown that Zn^{2+} is a potent inhibitor of these enzymes (4, 20, 45, 48). K_i values of *Hn*SOR were 46 μM for the oxygenase and 36 μM for the reductase activity, which are values comparable with the *Aa*SOR (Table 1) (48).

Structural properties of recombinant *H. neapolitanus* SOR. In order to compare the folding of mesophilic and (hyper)thermophilic SORs, we performed a circular dichroism (CD) study of the proteins from *H. neapolitanus* and *Acidianus ambivalens* (Fig. 4). The CD spectra of both proteins were rather similar, with minima around 220 nm and a shoulder at 209 nm (Fig. 4A). The low wavelength maximum of *Hn*SOR is not identifiable in the accessible spectral window. The signal intensity difference is likely due to quantification error. The conservation of spectral features suggests highly similar secondary structure content in both proteins. In addition, the hydrodynamic diameters as determined by dynamic light scattering were almost identical for both proteins (17.3 ± 1.0 nm for *Hn*SOR and 18.0 ± 0.8 nm for *Aa*SOR), showing that both proteins adopt comparable oligomeric states. *Hn*SOR was ~20°C less thermostable than the enzyme from the hyperthermophile (Fig. 4B).

3D modeling of the *H. neapolitanus* SOR. We performed homology modeling of the *Hn*SOR with the two *Acidianus* SOR structures as templates (Protein Data Bank [PDB] identifiers 2cb2 and 3bxv) (25, 46) in order to identify features that could give clues to the activity at low temperature and to temperature stability. The results obtained with the *H. neapolitanus* SOR were reproducible giving similar models, regardless of the modeling server and the template. When the modeled *Hn*SOR subunit was superimposed on each of the templates, the central beta barrel, the nine α-helices (longer than 5 amino acids [aa]) and the active site pocket were almost identical (Fig. 5A). Minor deviations were seen in loop or coil regions. The RMSD of the Cα chain was 0.16 to 0.38 Å.

The two *Acidianus* SORs are built from 24 subunits, each forming a large (15-nm-diameter) hollow sphere with a 432-point group symmetry and an almost impervious surface. The minimal building block is a subunit dimer, so that the holoenzymes repre-

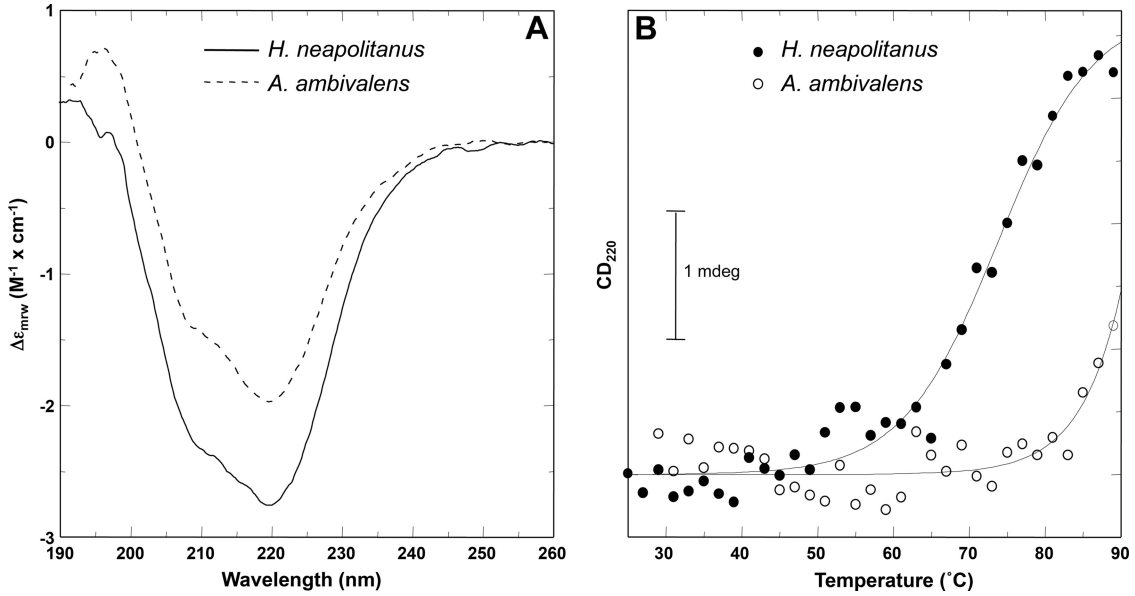

FIG 4 (A) Far-UV circular dichroism spectra of the SOR proteins from *Halothiobacillus neapolitanus* and *Acidianus ambivalens* at 0.1 mg/ml protein concentration and 25°C. (B) Thermal unfolding curves for the *H. neapolitanus* and *A. ambivalens* SOR, as measured from the CD variation at 220 nm. The lines show sigmoidal fits to the CD data. Values have been offset to facilitate comparison.

sent dodecamers of dimers (45, 46). The dynamic light scattering results suggest that the *Hn*SOR adopts a comparable multimerization state. When two of the modeled *Hn*SOR subunits were docked to each other, a dimer was formed, which could be superimposed on the *Aa*SOR structure with an RMSD of 1.7 Å (not shown).

Narrow pores at the 4-fold and 3-fold symmetry axes of the *Aa*SOR provide entrance to the inner cavity of the sphere (Fig. 5B and D). The question arose whether multimerization of the single subunit might lead to changes in the pore structures of the enzyme. When replacing one of the pore-forming subunits at the 4-fold symmetry axis of the *Aa*SOR with a copy of the modeled *Hn*SOR, changes in the pore structure became apparent. The phenylalanine residue F_{141} (in *Aa*SOR numbering) was conserved, which forms the outer ring of the two Phe rings. The inner Phe ring was not present due to replacement of F_{133} with a valine residue (Fig. 5B; see Fig. S1 in the supplemental material). In consequence, only one of the two access-restricting residues is retained in the *Hn*SOR.

The amino acids R_{99} and S_{226} define the pore at the 3-fold symmetry axis of the *Aa*SOR (Fig. 5D). They are connected by hydrogen bonds within and across the subunits. A salt bridge between R_{99} and E_{228} of the same subunit also might play a role in stabilization (48). Neither of these residues is conserved in the *Hn*SOR; R_{99} is replaced by a glutamate (E_{101}), S_{226} is replaced by A_{226} (see Fig. S1 in the supplemental material), and E_{228} is replaced by P_{228}. A_{226} defines the pore diameter when the modeled *Hn*SOR subunit was aligned to the pore-forming regions of the *Aa*SOR (Fig. 5C). E_{101} is predicted to form a hydrogen bond to the Nδ2 atom of N_{227}, whereas the Oδ2 atom of the same asparagine could form an H-bond to the Nζ atom of a lysine (K_{97}) of the neighboring subunit.

DISCUSSION

Sources of SORs or *sor* genes. Once thought to be restricted to some hyperthermophiles and thermophiles, the *sor* genes identified in genomes of mesophilic bacteria gave credit to a report by Tano and Imai from 1968 (43) on a SOR-like, glutathione-independent, and sulfur-dismutating enzyme activity in cell extracts of the bacterium *Acidithiobacillus thiooxidans* (formerly *Thiobacillus thiooxidans*). The sulfur-dismutating enzyme reaction was measured at 30°C in a Warburg apparatus. The products were H_2S and thiosulfate. These results were neither repeated nor confirmed, nor was the enzyme ever purified. In contrast, the GSH-dependent sulfur dioxygenases known from other acidithiobacilli represent a different and unrelated type of sulfur-oxidizing enzymes, which remained elusive so far (32, 42). Therefore, the molecular basis of sulfur oxidation in these microorganisms is not known despite their importance in bioleaching and formation of acid mine drainage (3). The preliminary shotgun genome sequence of *Acidithiobacillus thiooxidans* ATCC 19377 available at GenBank does not contain a *sor* homologue (GenBank accession number AFOH00000000.1). We chose *Halothiobacillus neapolitanus* (formerly *Thiobacillus neapolitanus*) as a representative mesophilic microbe carrying a SOR gene to demonstrate enzyme activity and to study the properties of the protein.

Like the two *Acidithiobacillus* species (Fig. 1), many but not all of the microorganisms with *sor* genes are (facultatively) chemolithoautotrophic sulfur oxidizers originating from sulfide or sulfur-rich springs, solfataras, or bioleaching environments. Others would not have been expected to carry a *sor* gene: for example, *Picrophilus torridus* is a thermoacidophile described as a strict heterotroph and *Desulfomicrobium baculatum* (formerly *Desulfovibrio baculatus*) is, as far as we know, a strictly anaerobic sulfate and sulfur reducer (34, 36). The physiological role of the SOR in these microorganisms is unknown.

***Hn*SOR activity within a broad pH and temperature range.** The *Hn*SOR is active over a broad pH range (pH 5.4 to 11) with an optimum at pH 8.4, when measured at 50°C. Measurements at the optimal temperature at alkaline pH were not possible because of the much higher rates of nonenzymatic sulfur disproportionation.

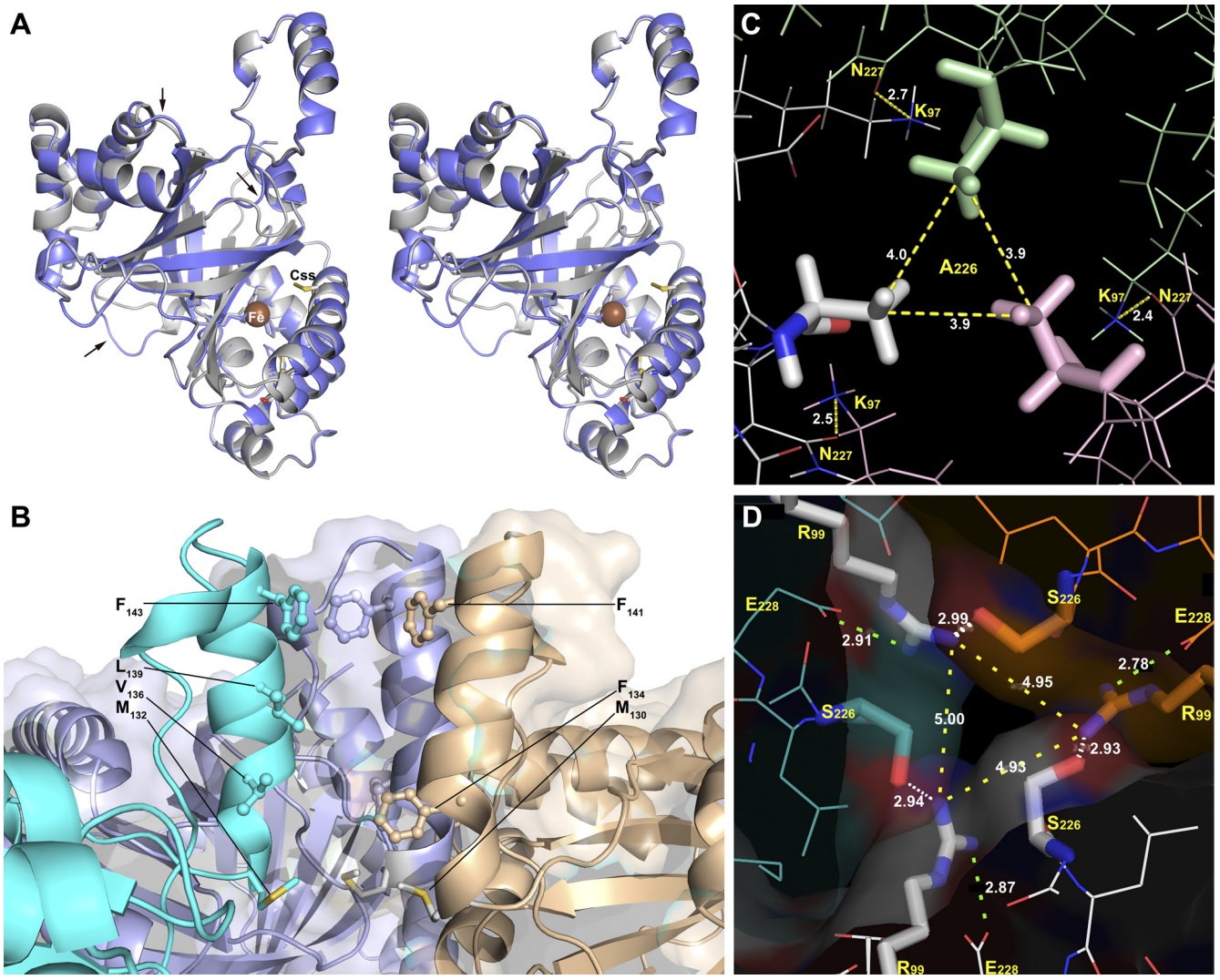

FIG 5 Three-dimensional modeling results of the *Hn*SOR amino acid sequence with the *Acidianus ambivalens* SOR (*Aa*SOR; PDB accession number 2cb2) as the template. (A) Cross-eyed stereo view of secondary structure representations of the modeled *Hn*SOR subunit structure (blue) superimposed on *Aa*SOR (gray). The iron atom (Fe) and cysteine persulfide (Css) are shown. The arrows indicate deviations in the coil regions. (B) Side view of the channel at the 4-fold symmetry axis showing two out of four *Aa*SOR subunits (purple and ochre), while the third subunit is replaced by the modeled *Hn*SOR subunit (cyan), including the outer (F_{141}) and inner (F_{133}) phenylalanine rings (*Aa*SOR only), the conserved methionine ring at its base (M_{130}), and valine and leucine residues in the *Hn*SOR. (C) Three copies of the modeled *Hn*SOR subunit aligned to the respective *Aa*SOR subunits (shown in panel D) at the 3-fold symmetry axis showing the channel-forming residues with the distances in angstroms (yellow broken lines and small white numbers) and the putative hydrogen bonds between K_{97}, N_{227}, and E_{101}. (D) Channel at the 3-fold symmetry axis of the *Aa*SOR formed by R_{99} and S_{226}. Distances are given between the Nη atoms of the arginines (yellow dashes), for the salt bridges to E_{228} (green dashes), and for the hydrogen bond to the Oγ of the S_{226} of the neighboring subunit (white dashes). Panel D reprinted from reference 48 with permission of the publisher.

The pH range of the *Hn*SOR extends further into the alkaline region than for any of the SORs characterized so far (Table 1) (4, 20, 30, 41). The pH preference correlates with the slightly alkaline internal pH of *H. neapolitanus* (pH of ≈7.8) (44). In contrast, the pH optimum of the *Aa*SOR is 7 to 7.4, correlating with an internal pH of around 6.5 (28).

The enzymatic activity of the *Hn*SOR covered a temperature span of almost 90 K, ranging from 10°C to 99°C (Fig. 3), which makes it a thermozyme. Two questions arise from these observations, namely, how the protein maintains its thermostability and how flexibility is retained sufficiently at low temperatures and low substrate concentrations to enable catalysis.

Even though the *Hn*SOR originates from a mesophilic microorganism with an optimal growth temperature around 30°C (maximum 42°C) (17), both oxygenase and reductase activities peaked at 80°C. As a comparison, the SOR from the hyperthermophile *Ac. ambivalens* (maximal growth temperature of 88°C) was active from 50°C to 108°C (Table 1) (20, 52). Despite the structural similarity between the enzymes from the hyperthermophile and mesophile observed by spectroscopy, the distinct environmental conditions of the organisms result in specific adaptations, including the level of stability and their catalytic properties. High environmental temperatures impose the need for thermostabilization of the enzymes, resulting in a higher rigidity, less flexibility and low or no activity at ambient temperatures (50). However, when the comparison is done at their respective optimal catalytic

temperature, the enzymes tend to have identical flexibilities under their particular optimal working conditions so that a "corresponding state" is maintained regarding conformational flexibility (50). The *Hn*SOR is a remarkable exception to this well-established trend. In fact, the specific *Hn*SOR activity exceeded the (hyperthermophilic) *Aa*SOR activity about 10-fold under optimal conditions (20, 45, 48).

The second question to be answered was about the factors that make the *Hn*SOR active at low temperatures. We had observed that the enzyme should be partially melted at the optimal reaction temperature. The apparent thermal stability was about 20 K lower than the *Aa*SOR (Fig. 4B). The results suggest that the *Hn*SOR has a higher flexibility compared to the more rigid *Aa*SOR, which is not active below 50°C (20). The results also suggest that the thermal denaturation is reversible; however, these conclusions have not yet been verified independently by other methods.

In addition, we had shown in a previous study that the widths of the pores at the 4-fold and 3-fold symmetry axes are crucial for specific *Aa*SOR activities: the wider the pores are, the higher the activity becomes (48). In this context, the changes seen in the pores of the outer shell of the *Hn*SOR (Fig. 5B to D) suggest that the barriers are less restrictive: at the 4-fold axis, the inner ring of the two Phe rings is missing. At the 3-fold axis, the salt bridge-forming arginine and glutamate residues are not present, while the H-bond-forming serine is replaced in favor of an alanine. This should be flexible enough to allow easy passage of substrate and/or products. In the *Hn*SOR, a novel and wider hydrogen-bonding network centered at N_{227} replaced the salt bridges (and the hydrogen bonds provided by S_{226} [Fig. 5C and D]) that are considered to stabilize subunit interactions and confer rigidity to the 3-fold axis of the *Aa*SOR.

SORs are structurally conserved. The difference of 40 to 50°C between the maximal or optimal growth temperature and the enzyme activity optimum is much higher than what would have been expected from the overall protein stability. The question of how this came about may be tentatively explained by one (or more) of the following hypotheses. (i) The high optimal temperature of *Hn*SOR is a trait that persisted (e.g., *Aa*SOR) due to lack of evolutionary pressure. (ii) The activity-temperature profile is a consequence of the coupling between enzyme activity and protein structure: any SOR protein will have such a high optimal temperature and intrinsic thermostability. (iii) The existence of *Hn*SOR activity over broad pH and temperature ranges is an adaptive mechanism, which allows metabolic homeostasis upon environmental changes. Comparison of the biochemical properties and the sequences (Table 1; see Fig. S1 in the supplemental material) suggests that the SORs have similar properties independent of adaptations to the host organism.

We used spectroscopy and a homology modeling approach to make some predictions regarding the reasons for the thermostability and temperature range of the enzyme. The different catalytic properties of *Hn*SOR and *Aa*SOR do not reside in major differences in the secondary structure content. The similar far-UV CD spectra indicated that the overall fold is preserved among enzymes from mesophilic and thermophilic microorganisms (Fig. 4A). This interpretation is supported by the modeling results, which showed little changes in the main secondary structure features of the subunit (Fig. 5A). In addition, the oligomeric assembly also seems to be conserved, as noted from the similar hydrodynamic properties of both enzymes. The slightly larger hydrodynamic diameter compared to the diameter obtained by electron microscopy and X-ray crystallography (≈15 nm [20, 25, 45, 46]) reflects the conformational dynamics in solution, the effect of the solvation shell, and the averaging inherent in an ensemble measurement.

SORs feature conserved amino acid sequences regardless whether they originate from mesophilic or hyperthermophilic microorganisms (see Fig. S1 in the supplemental material). Consequently, the basic building blocks are conserved in the available 3D structures and in the models, which includes the central beta barrel with the surrounding alpha helices (PDB identifiers 2cb2 and 3bxv). This suggests that they are core features that make the proteins resistant against thermal melting of the subunits, even if the individual denaturation temperatures might vary (Fig. 4B).

Subunit interactions are another important parameter for thermostability. It has long been known that hollow spheres are intrinsically stable regardless of whether they are macroscopic objects (37), small molecules like fullerenes (23), or large protein complexes like ferritins. Ferritins are intrinsically thermostable and adopt a comparable quaternary structure of 24 subunits in 432-point group symmetry (12, 13, 39). The 24 subunits of SORs are assembled from dimers (45, 46), again a feature similar to ferritins (39). Docking experiments with the modeled subunits showed that dimer formation is feasible. The fit was not optimal but was in good correlation with the template. Taken together, the results suggest that these features—thermostable subunits, dimer formation, and oligomerization to yield the 24-mer—are common and intrinsic properties of the SORs in general (hypothesis ii).

Conclusion. SORs were once thought to be restricted to some hyperthermophiles and thermophiles, because the enzyme activity had not been recognized in mesophiles with one exception (43). The data presented here showed that the *Hn*SOR possesses folding and quaternary structure properties similar to the SORs from (hyper)thermophiles. However, the activity at low temperatures seems to result from a combination of a less thermostable and more flexible oligomer with less restrictive access. In the context of the limited bioavailability of sulfur at mesophilic temperatures, the basal activity and flexibility of the *Hn*SOR effectively contribute to adequate metabolic flows of sulfur metabolites for the microorganism.

ACKNOWLEDGMENTS

We thank Felicitas Pfeifer (Darmstadt, Germany) for her generosity and encouragement.

A. Veith and A. Kletzin were supported by a grant from the Deutsche Forschungsgemeinschaft (Az Kl885-6/1).

REFERENCES

1. **Boden R, et al.** 21 August 2011. Phylogenetic assessment of culture collection strains of *Thiobacillus thioparus*, and definitive 16S rRNA gene sequences for *T. thioparus*, *T. denitrificans*, and *Halothiobacillus neapolitanus*. Arch. Microbiol. doi:10.1007/s00203-011-0747-0. [Epub ahead of print.]
2. **Bradford MM.** 1976. A rapid and sensitive method for the quantitation of microgram quantities of protein utilizing the principle of protein-dye binding. Anal. Biochem. **72**:248–254.
3. **Brandl H.** 2001. Microbial leaching of metals, p 191–224. *In* Rehm HJ (ed), Biotechnology, vol 10. Special processes. Wiley-VCH, Weinheim, Germany.
4. **Chen ZW, Jiang CY, She Q, Liu SJ, Zhou PJ.** 2005. Key role of cysteine residues in catalysis and subcellular localization of sulfur oxygenase-

reductase of *Acidianus tengchongensis.* Appl. Environ. Microbiol. **71**: 621–628.
5. **Chen ZW, et al.** 2007. Novel bacterial sulfur oxygenase reductases from bioreactors treating gold-bearing concentrates. Appl. Microbiol. Biotechnol. **74**:688–698.
6. **Comeau SR, Gatchell DW, Vajda S, Camacho CJ.** 2004. ClusPro: a fully automated algorithm for protein-protein docking. Nucleic Acids Res. **32**: W96–W99.
7. **DeLano WL.** 2002. The PyMOL Molecular Graphics System, 0.97 ed. DeLano Scientific, San Carlos, CA.
8. **Emmel T, Sand W, König WA, Bock E.** 1986. Evidence for the existence of a sulfur oxygenase in *Sulfolobus brierleyi.* J. Gen. Microbiol. **132**: 3415–3420.
9. **Fischer DS, Price DC.** 1964. Simple serum iron method using new sensitive chromogen tripyridyl-s-triazine. Clin. Chem. **10**:21–25.
10. **Friedrich CG, Bardischewsky F, Rother D, Quentmeier A, Fischer J.** 2005. Prokaryotic sulfur oxidation. Curr. Opin. Microbiol. **8**:253–259.
11. **He Z, Li Y, Zhou P, Liu S.** 2000. Cloning and heterologous expression of a sulfur oxygenase/reductase gene from the thermoacidophilic archaeon *Acidianus* sp. S5 in *Escherichia coli*. FEMS Microbiol. Lett. **193**:217–221.
12. **Janner A.** 2008. Comparative architecture of octahedral protein cages. I. Indexed enclosing forms. Acta Crystallogr. Sect. A **64**:494–502.
13. **Janner A.** 2008. Comparative architecture of octahedral protein cages. II. Interplay between structural elements. Acta Crystallogr. Sect. A **64**: 503–512.
14. **Janosch C, et al.** 2009. Sulfur oxygenase reductase in different *Acidithiobacillus caldus*-like strains. Adv. Materials Res. **71–73**:239–243.
15. **Kamyshny A.** 2009. Solubility of cyclooctasulfur in pure water and sea water at different temperatures. Geochim. Cosmochim. Acta **73**: 6022–6028.
16. **Kelley LA, Sternberg MJ.** 2009. Protein structure prediction on the Web: a case study using the Phyre server. Nat. Protoc. **4**:363–371.
17. **Kelly DP, Wood AP.** 2005. *Halothiobacillus*, p 58–59. *In* Brenner DJ, Krieg NR, Staley JT, Garrity GM (ed), Bergey's manual of systematic bacteriology, 2nd ed, vol 2. Springer, New York, NY.
18. **Kelly DP, Wood AP.** 2000. Reclassification of some species of *Thiobacillus* to the newly designated genera *Acidithiobacillus* gen. nov., *Halothiobacillus* gen. nov. and *Thermithiobacillus* gen. nov. Int. J. Syst. Evol. Microbiol. **50**(Part 2):511–516.
19. **Kletzin A.** 2008. Oxidation of sulfur and inorganic sulfur compounds in *Acidianus ambivalens*, p 184–201. *In* Dahl C, Friedrich CG (ed), Microbial sulfur metabolism. Springer, Berlin, Germany.
20. **Kletzin A.** 1989. Coupled enzymatic production of sulfite, thiosulfate, and hydrogen sulfide from sulfur: purification and properties of a sulfur oxygenase reductase from the facultatively anaerobic archaebacterium *Desulfurolobus ambivalens.* J. Bacteriol. **171**:1638–1643.
21. **Kletzin A.** 1992. Molecular characterization of the *sor* gene, which encodes the sulfur oxygenase reductase of the thermoacidophilic archaeon *Desulfurolobus ambivalens.* J. Bacteriol. **174**:5854–5859.
22. **Kozakov D, et al.** 2010. Achieving reliability and high accuracy in automated protein docking: ClusPro, PIPER, SDU, and stability analysis in CAPRI rounds 13–19. Proteins **78**:3124–3130.
23. **Kroto HW.** 1987. The stability of the fullerenes C-24, C-28, C-32, C-36, C-50, C-60 and C-70. Nature **329**:529–531.
24. **Lassmann T, Sonnhammer EL.** 2005. Kalign–an accurate and fast multiple sequence alignment algorithm. BMC Bioinformatics **6**:298.
25. **Li M, et al.** 2008. Crystal structure studies on sulfur oxygenase reductase from *Acidianus tengchongensis.* Biochem. Biophys. Res. Commun. **369**: 919–923.
26. **Mangold S, Valdés J, Holmes D, Dopson M.** 2011. Sulfur metabolism in the extreme acidophile *Acidithiobacillus caldus.* Front. Microbiol. **2**:17.
27. **McIlvaine TC.** 1921. A buffer solution for colorimetric comparison. J. Biol. Chem. **49**:183–186.
28. **Moll R, Schäfer G.** 1988. Chemiosmotic H+ cycling across the plasma membrane of the thermoacidophilic archaebacterium *Sulfolobus acidocaldarius.* FEBS Lett. **232**:359–363.
29. **Parker CD.** 1947. Species of sulphur bacteria associated with the corrosion of concrete. Nature **159**:439.
30. **Pelletier N, Leroy G, Guiral M, Giudici-Orticoni MT, Aubert C.** 2008. First characterisation of the active oligomer form of sulfur oxygenase reductase from the bacterium *Aquifex aeolicus.* Extremophiles **12**:205–215.
31. **Pettersen EF, et al.** 2004. UCSF Chimera–a visualization system for exploratory research and analysis. J. Comput. Chem. **25**:1605–1612.
32. **Rohwerder T, Sand W.** 2003. The sulfane sulfur of persulfides is the actual substrate of the sulfur-oxidizing enzymes from *Acidithiobacillus* and *Acidiphilium* spp. Microbiology **149**:1699–1710.
33. **Roy AB, Trudinger PA.** 1970. The chemistry of some sulphur compounds, p 7–29. *In* Roy AB, Trudinger PA (ed), The biochemistry of inorganic compounds of sulphur. Cambridge University Press, Cambridge, United Kingdom.
34. **Rozanova EP, Nazina TN.** 1976. Mesophilic rod-like nonsporeforming bacterium reducing sulfates. Mikrobiologiia **45**:825–830. (In Russian.)
35. **Schägger H, von Jagow G.** 1987. Tricine-sodium dodecyl sulfate-polyacrylamide gel electrophoresis for the separation of proteins in the range from 1 to 100 kDa. Anal. Biochem. **166**:368–379.
36. **Schleper C, et al.** 1995. *Picrophilus* gen. nov., fam. nov.: a novel aerobic, heterotrophic, thermoacidophilic genus and family comprising archaea capable of growth around pH 0. J. Bacteriol. **177**:7050–7059.
37. **Schwerin E.** 1922. Zur Stabilität der dünnwandigen Hohlkugel unter gleichmäßigem Außendruck. Z. Angew. Math. Mechanik **2**:81–91.
38. **Skerra A.** 1994. Use of the tetracycline promoter for the tightly regulated production of a murine antibody fragment in *Escherichia coli.* Gene **151**: 131–135.
39. **Stefanini S, et al.** 1996. Thermal stability of horse spleen apoferritin and human recombinant H apoferritin. Arch. Biochem. Biophys. **325**:58–64.
40. **Steudel R.** 2003. Inorganic polysulfanes H_2S_n with $n > 1$. Top. Curr. Chem. **231**:99–125.
41. **Sun CW, Chen ZW, He ZG, Zhou PJ, Liu SJ.** 2003. Purification and properties of the sulfur oxygenase/reductase from the acidothermophilic archaeon, *Acidianus* strain S5. Extremophiles **7**:131–134.
42. **Suzuki I.** 1965. Oxidation of elemental sulfur by an enzyme system of *Thiobacillus thiooxidans.* Biochim. Biophys. Acta **104**:359–371.
43. **Tano T, Imai K.** 1968. Physiological studies on thiobacilli. Part II. The metabolism of colloidal sulfur by the cell-free enzyme system of *Thiobacillus thiooxidans.* Agric. Biol. Chem. **32**:51–54.
44. **Tsai Y, et al.** 2007. Structural analysis of CsoS1A and the protein shell of the *Halothiobacillus neapolitanus* carboxysome. PLoS Biol. **5**:e144.
45. **Urich T, et al.** 2004. The sulphur oxygenase reductase from *Acidianus ambivalens* is a multimeric protein containing a low-potential mononuclear non-haem iron centre. Biochem. J. **381**:137–146.
46. **Urich T, Gomes CM, Kletzin A, Frazao C.** 2006. X-ray structure of a self-compartmentalizing sulfur cycle metalloenzyme. Science **311**: 996–1000.
47. **Urich T, et al.** 2005. Identification of core active site residues of the sulfur oxygenase reductase from *Acidianus ambivalens* by site-directed mutagenesis. FEMS Microbiol. Lett. **248**:171–176.
48. **Veith A, et al.** 2011. Substrate pathways and mechanisms of inhibition in the sulfur oxygenase reductase of *Acidianus ambivalens.* Front. Microbiol. **2**:37.
49. **Wood AP, Woodall CA, Kelly DP.** 2005. *Halothiobacillus neapolitanus* strain OSWA isolated from "The Old Sulphur Well" at Harrowgate (Yorkshire, England). Syst. Appl. Microbiol. **28**:746–748.
50. **Zavodszky P, Kardos J, Svingor Petsko GA.** 1998. Adjustment of conformational flexibility is a key event in the thermal adaptation of proteins. Proc. Natl. Acad. Sci. U. S. A. **95**:7406–7411.
51. **Zhang Y.** 2008. I-TASSER server for protein 3D structure prediction. BMC Bioinformatics. **9**:40.
52. **Zillig W, et al.** 1986. *Desulfurolobus ambivalens* gen. nov., sp. nov., an autotrophic archaebacterium facultatively oxidizing and reducing sulfur. Syst. Appl. Microbiol. **8**:197–203.

The Sulfur Oxygenase Reductase from the Mesophilic Bacterium *Halothiobacillus neapolitanus* is a Highly Active Thermozyme

Supplementary Material

Andreas Veith[1], Hugo M. Botelho[2], Florian Kindinger[1], Cláudio M. Gomes[2] and Arnulf Kletzin*[1]

[1]Institute of Microbiology and Genetics, Technische Universität Darmstadt, Darmstadt, Germany
[2]Instituto de Tecnologia Química e Biológica. Universidade Nova de Lisboa. Av. da República, EAN. 2785-572 Oeiras, Portugal

***Correspondence:**

Dr. Arnulf Kletzin
Institute of Microbiology and Genetics
Technische Universität Darmstadt
Schnittspahnstraße 10
64287 Darmstadt, Germany
Kletzin@bio.tu-darmstadt.de
Phone +49 6151 16-5254

Supplementary figure S1 (following page): Multiple alignment of the SOR sequences available in public databases. Genbank identification (GI) numbers are given at the end; *derived from the genome sequences available at the Joint Genome Institute (http://www.jgi.doe.gov). The horizontal line separates Archaea from Bacteria below. Black bar, chimney-like protrusion at the four-fold symmetry axes with the residues forming the two phenylalanine rings in the *Aa*SOR; cylinders, α-helices; arrows, beta sheets; light green cylinder, additional α-helix in the *Aquifex* SOR; abbreviations: Css, cysteine persulfide; Fe, iron-coordinating residues; Zn, zinc-binding residues; other residues are discussed in the Homology Modeling section (Fig. 5); residues above the alignment, *Aa*SOR; residues below the alignment, *Hn*SOR.

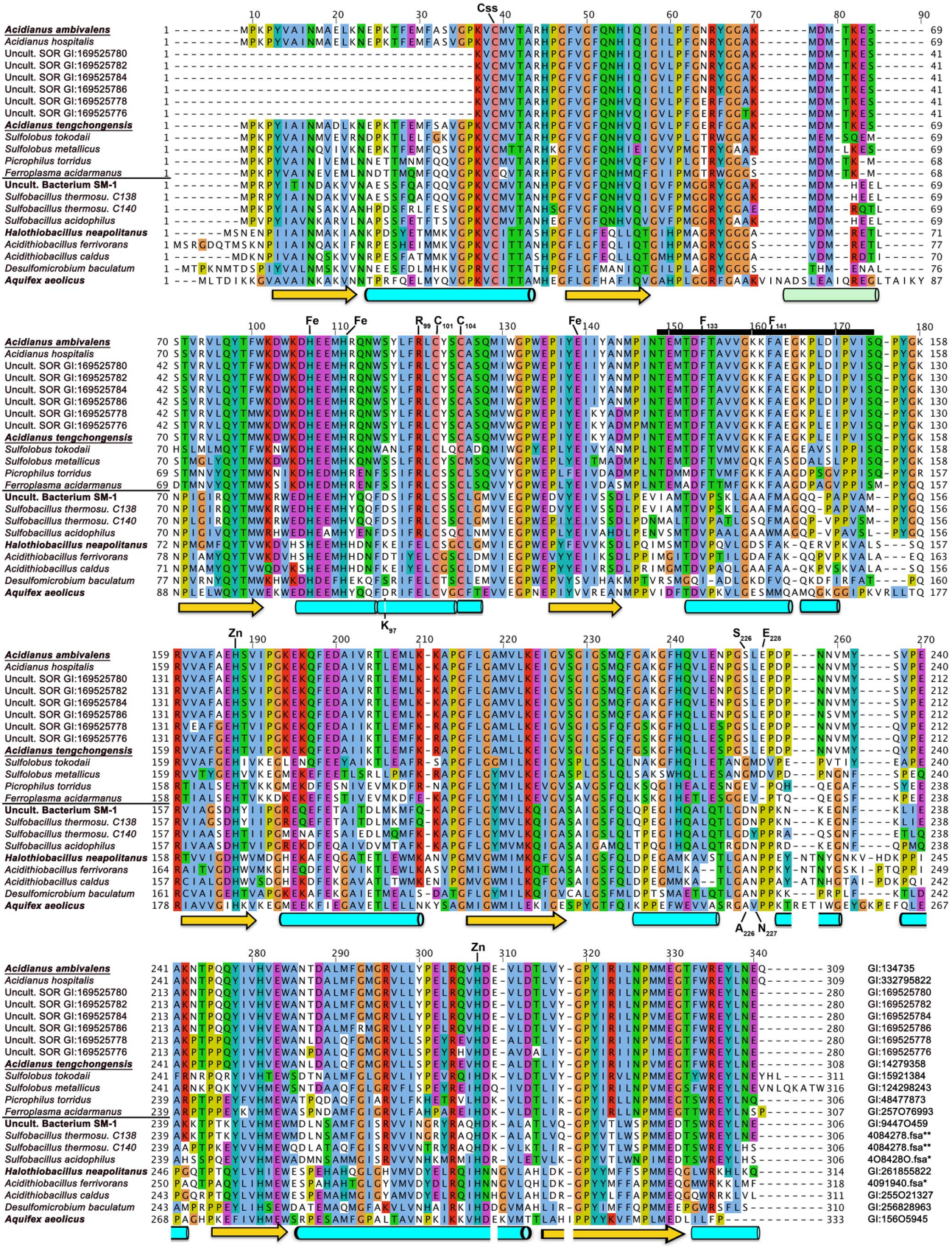
Css
Fe
Fe
R99
C101
C104
Fe
F133
F141
Zn
K97
S226
E228
A226
N227
Zn

41
42
43